

Supporting Information

For

Rheology of Novel Cellulose Ethers Excipients Designed for Hot Melt Extrusion

Tirtha Chatterjee^{*1}, Kevin P. O'Donnell², Mark A. Rickard³, Brian Nickless⁴,
Yongfu Li³, Valeriy V. Ginzburg⁴, Robert L. Sammler⁴

¹Dow Water & Process Solutions, The Dow Chemical Company, Collegetown, PA 19426

²Dow Pharma, Food & Medical, The Dow Chemical Company, Midland, MI 48674

³Analytical Sciences, Core R&D, The Dow Chemical Company, Midland, MI 48667

⁴Materials Science and Engineering, Core R&D, The Dow Chemical Company, Midland, MI 48674

[*tchatterjee@dow.com](mailto:tchatterjee@dow.com)

S1: Size Exclusion Chromatography (SEC)

SEC system was based on a Waters 2695 LC pump and autosampler that was equipped with a filter consisting of one layer of 0.1- μm nylon membrane, installed prior to the injection valve. Flow rate was set at 1.0 mL/min, and the injection volume was 100 μL of solution. SEC separation was carried out using two TOSOH GMPW columns having 7.5 mm i.d. x 300 mm length (nominal particle size 17 μm and pore size 100-1000 \AA) operated at 28 $^{\circ}\text{C}$. SEC eluent was 0.05 wt% NaN_3 water solution that has been recirculated through a 0.04- μm nylon cartridge for about 6 hours to remove particulate impurity. The detectors were a Wyatt DAWN HELEO II multi-angle laser light scattering (MALLS) detector and a Wyatt Optilab TrEX differential refractive index (DRI) detector. The Wyatt DAWN was equipped with a red laser operating at a wavelength of 660 nm at ambient temperature, and a TrEX DRI detector equipped with a light emitting diode (LED) having the same wavelength as that of DAWN (660 nm) and operated at 28 $^{\circ}\text{C}$.

The Wyatt DAWN MALLS was calibrated with HPLC-grade toluene filtered through a 0.05- μm syringe filter. The individual light scattering detectors were normalized to the 90 $^{\circ}$ light-scattering detector using mono-dispersed bovine serum albumin (BSA) monomer as the isotropic scatter. The inter-detector delay volume was determined by aligning the 90 $^{\circ}$ light scattering and DRI peaks obtained for BSA.

The signals from the MALLS and DRI detectors were analyzed using ASTRA 6 software, version 6.1. Molecular weights were determined at each SEC elution volume increment. To obtain these metrics, Debye plots covering the angular range from 25.8° to 132.2° were least-squares fit to a first order polynomial according to the Zimm formalism. A dn/dc of 0.140 mL/g for all HPMC samples was used.¹ Reported molecular weight averages and radii of gyration were based on the first-order exponential fitting of slice M and R_g from ASTRA 6 software. Mass recovery was obtained by comparing the detected mass from integration of the DRI signal to the injected mass.

Determination of Persistence Lengths (l_p): The dependence of the weight-average radius-of-gyration $R_{g,w}$ on absolute molecular weight M is shown in Figure S1. Power-law slopes ($d\ln(R_{g,w})/d\ln M$) of the data were estimated from a linear regression of the data on double logarithmic axes for the highest- M chains ($M > 10^4$ g/mol) in the experimental window, and are tabulated in the figure for the three materials. The slopes are very similar (0.5) for the two higher- M materials (100 and 4M cP) and indistinguishable from that (0.5) expected at the theta-solvent limit. Such a low slope indicates the chains are in a thermodynamically poor solvent, and may be expected for cellulosic materials with high levels of the (methylether) hydrophobic side chains. A much lower slope (0.32) is observed for the lowest- M material, and the origin of this weaker slope is not well understood.

The persistence length l_p of the two higher- M materials was estimated from the data in Figure S1 based on the functional form ($R_{g,w}^2 = (1/3)l_p L - l_p^2 + 2 l_p^3/L + (2 l_p^4/L^2)[\exp(-l_p/L) - 1]$) postulated by Kratky and Porod.²⁻³ Here, the chain contour length $L (= a \cdot (M/M_0))$ is assumed proportional to the degree of polymerization (M/M_0) and the length ($a = 0.7$ nm) of the anhydroglucose repeat unit. The model function fit to data is excellent as illustrated by the broken-line curves in Figure S1. The persistence lengths are found to be about half that (13.3 ± 0.3 nm)⁴ of a lower-substituted cellulosic ether material (methyl cellulose, $DS = 1.86 \pm 0.03$ mol MeO/mol AGU) measured with the same SEC approach. The data are consistent with the expectation that the chain backbone stiffness arises from hydrogen bonding between adjacent repeat units, and that level of hydrogen (and backbone stiffness) will decrease as the backbone OH groups are annihilated by reactions grafting (MeO and HPO) side chains to the backbone. No attempt was made to estimate l_p for the low- M material since the functional form of Kratky and Porod will not be able to fit a power-law slope of 0.32.

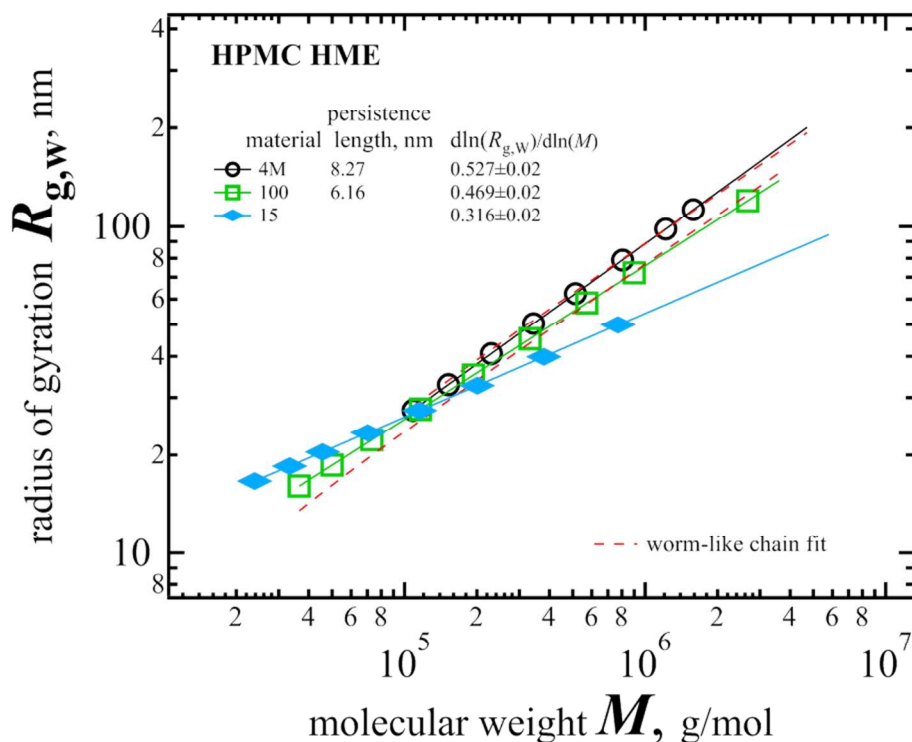


Figure S1: Dependence of the weight-average radius-of-gyration $R_{g,w}$ on absolute molecular weight M for three HPMC HME materials measured at 27 °C in the aqueous SEC mobile phase. Markers are sparsely placed on each continuous-looking curve to identify the material. The data were fit with the worm-like chain model (- - -) to estimate the persistence length (l_p).

Translation of the backbone stiffness (or l_p) measured at dilute aqueous solvated conditions into backbone stiffness at HME conditions remains an open question. A lower l_p suggests increased backbone flexibility likely arising from partial removal of intramolecular hydrogen bonding (hydrogen bonding between adjacent repeat units) through substitutions. In contrast, high-temperature vibrational spectroscopy (See Figure 8 in the main text or Figure S5 in this document) revealed the presence of finite amount of hydrogen bonding even at elevated temperatures (HME conditions). One possibility is increased backbone flexibility perhaps enables the formation of intermolecular hydrogen bonds (e.g. hydrogen bonds between the OH groups on the ends of the HPO side chains and the oxygen atoms on the anhydroglucose backbone) that are absent in pure cellulose or in their methyl ether derivatives.

S2: Melt rheology of general purpose polystyrene (GPPS) 666

The temperature dependent rheology of a common glassy polymer having a similar glass transition temperature was conducted to describe typical rheological behavior of a conventional entangled polymers

at temperatures above its glass transition. The selected polymer was general-purpose polystyrene (GPPS) 666 [melt-flow and T_g are 8.0 g/10 min (at 200 °C under 5kg load) and 104 °C, respectively]. At 140 °C, about 35 °C above the T_g , a clear G' and G'' cross-over was observed at a frequency, ω of about 0.04 rad/s as shown in Figure S2a. This crossover progressively moved to higher frequency (or shorter time) at elevated temperatures ($\omega \sim 1.6$ and 10 rad/s at 170 and 190 °C, respectively). Beyond the crossover typical liquid-like terminal rheology scaling⁵ (as $\omega \rightarrow 0$, $G' \sim \omega^2$ and $G'' \sim \omega^1$) was reached. Terminal rheology scaling indicates complete relaxation of polymer chains and attainment of zero-shear viscosity.

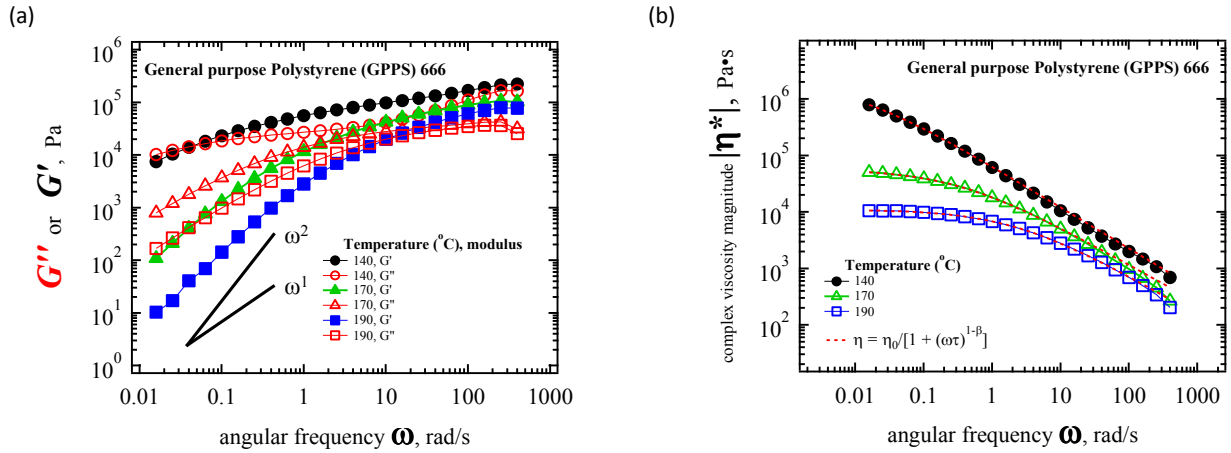


Figure S2: Dependence of small-amplitude oscillatory shear flow viscoelastic data on the oscillation frequency for general purpose polystyrene (GPPS) 666 polymer at different temperatures. The frequency dependent shear storage (G') and loss (G'') moduli data are shown in plot (a) and the magnitude component of the complex viscosity data are shown in plot (b). The dotted red lines in plot (b) represent Cross model fit to the complex viscosity data.

The zero-shear viscosity for the GPPS 666 can be extracted by fitting Cross model⁶ to complex viscosity data (Figure S2b) given as:

$$|\eta^*| = \frac{\eta_0}{[1+(\omega\tau)^{1-\beta}]} \quad (1)$$

where $|\eta^*|$ is the magnitude component of the complex viscosity, η_0 is the zero-shear viscosity, τ is a characteristic relaxation time and β is the parameter that controls the steepness of viscosity reduction as a function of frequency. The η_0 values were found to be $(1.9 \pm 0.1) \times 10^5$, $(4.8 \pm 0.3) \times 10^4$, and $(1.1 \pm 0.3) \times 10^4$ Pa-s at 140, 170 and 190 °C, respectively. The corresponding characteristic relaxation time scales were 100.0 ± 12.7 , 1.9 ± 0.4 and 0.5 ± 0.1 s, respectively. The typical β value was 0.25 ± 0.01 . These values are tabulated in Table S1.

Table S1. Cross model fit parameters to the GPPS 666 complex viscosity data obtained from dynamic frequency sweep measurements at different temperatures. The T_g of the GPPS 666 polymer is 104 °C.

Temperature (°C)	η_0 (Pa-s)	τ (s)	β
140	$(1.9 \pm 0.1) \times 10^5$	100.0 ± 12.7	0.25 ± 0.03
170	$(4.8 \pm 0.3) \times 10^4$	1.9 ± 0.4	0.24 ± 0.03
190	$(1.1 \pm 0.3) \times 10^4$	0.5 ± 0.1	0.26 ± 0.03

Rheological properties of polymer melts and solutions generally do not depend on the sample preparation steps or flow and time history. Such fluids are categorized as rheologically simple systems. One way to define a rheologically simple system is if viscosity data measured at the same temperature in linear oscillatory shear flows and in steady nonlinear shear flows will superpose when plotted in the special format recommended by Cox and Merz.⁷ More specifically, one measures the dependence of the complex viscosity $\eta^*(\omega)$ on oscillation frequency ω and the dependence of the steady-state shear viscosity $\eta(\dot{\gamma})$ on shear strain rate $\dot{\gamma}$, and labels the system as rheologically simple when the $|\eta^*(\omega)|$ versus ω data superposes the $\eta(\dot{\gamma})$ versus $\dot{\gamma}$ data. The Cox-Merz empiricism was found to be valid for general purpose polystyrene (GPPS) 666 at 170 and 190 °C. A representative plot along with fit to Cross model is shown in Figure S3.

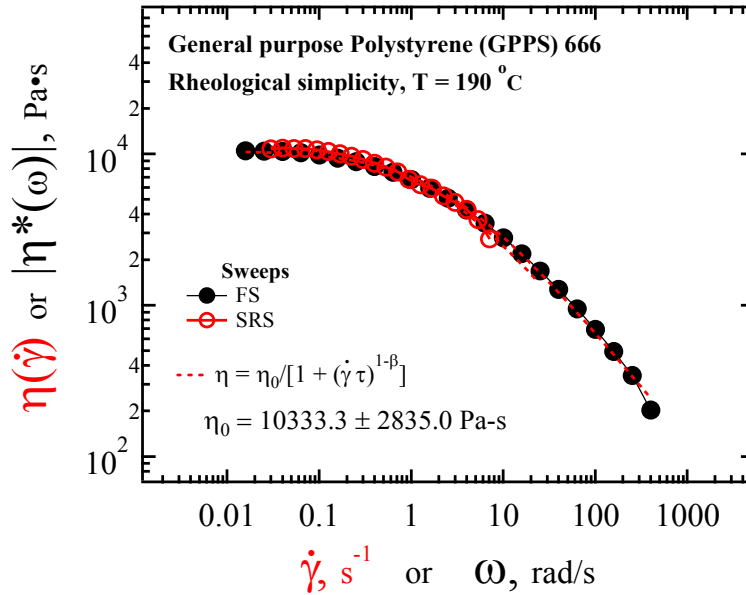


Figure S3: Comparison of oscillatory- and steady-shear viscosity in Cox-Merz formalism for General purpose polystyrene (GPPS) 666 at 190 °C. FS stands for frequency sweep (under oscillatory shear) and SRS stands for strain rate sweep (under steady shear). The dotted line represents Cross model fit to data.

S3: Attempt to measure yield stress using rotational rheometers: Stress amplitude sweep data

An attempt was made to measure the yield stress, σ_Y , directly using a stress-controlled AR-G2 rheometer with the sample warmed to the target temperature with a Peltier-controlled lower plate. A fresh aliquot (25-mm diameter circular disc specimen) was subjected to stress amplitude sweep at 170 °C with the applied oscillatory shear stress range from 0.1 to 6.5×10^4 Pa. Note that 6.5×10^4 Pa is the upper stress limit for the AR-G2 rheometer. For the entire stress range HPMC HME polymers were found to be solid-like with $G' \gg G''$ and both moduli were independent of stress (linear viscoelasticity) (Figure S4). Therefore, one can infer that at 170 °C, the σ_Y must be above 6.5×10^4 Pa and their measurement is experimentally inaccessible using a commercial rotational rheometer.

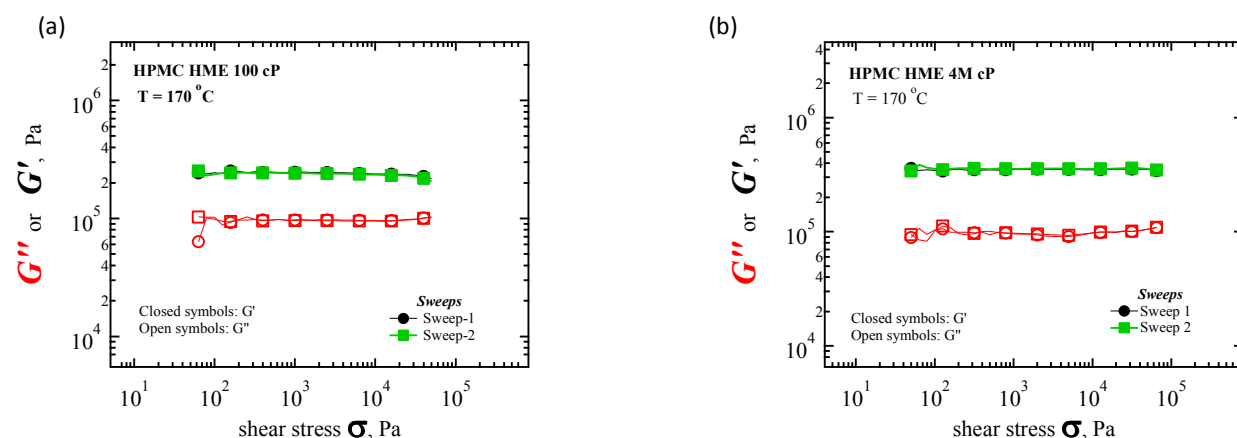
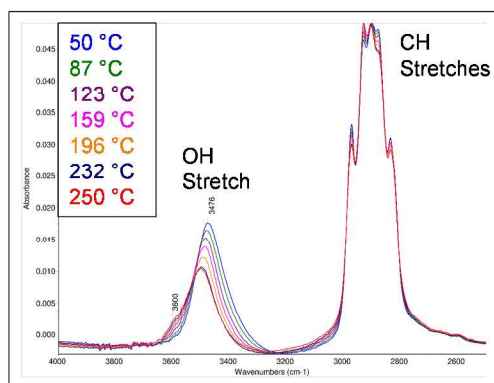


Figure S4: Stress-amplitude sweep under oscillatory shear at 170 °C for HPMC HME (a) 100- and (b) 4M cP polymers. Both samples showed linear viscoelasticity (i.e. both the moduli were independent of the applied stress amplitude) for the entire stress window.

S4: Infrared spectra of HPMC HME

(a)



(b)

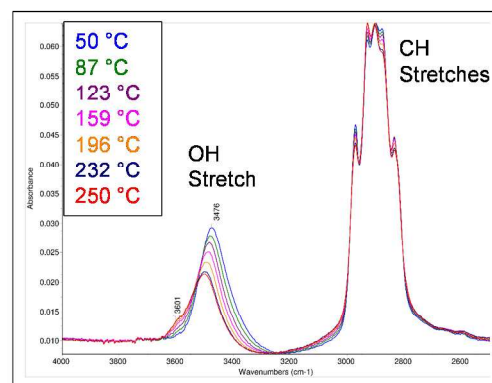


Figure S5: Infrared spectra of HPMC HME (a) 15- and (b) 4M cP grades from 50 to 250 °C covering the OH and CH stretches regions. Spectra were collected while warming the sample at a 10 °C/min rate.

References

1. Li, Y. F.; Shen, H. W.; Lyons, J. W.; Sammler, R. L.; Brackhagen, M.; Meunier, D. M., Size-exclusion chromatography of ultrahigh molecular weight methylcellulose ethers and hydroxypropyl methylcellulose ethers for reliable molecular weight distribution characterization. *Carbohydr Polym* **2016**, *138*, 290-300.
2. Kirste, R. G.; Oberthur, R. C., Synthetic Polymers in Solutions. In *Small Angle X-ray Scattering*, Glatter, O.; Kratky, O., Eds. Academic Press: London, 1982; pp 387-431.
3. Kratky, O.; Porod, G., Röntgenuntersuchung gelöster Fadenmoleküle. *Rec. Trav. Chim. Pays-Bas*. **1949**, *68*, 1106-1123.
4. Chatterjee, T.; Nakatani, A. I.; Adden, R.; Brackhagen, M.; Redwine, D.; Shen, H. W.; Li, Y. F.; Wilson, T.; Sammler, R. L., Structure and Properties of Aqueous Methylcellulose Gels by Small-Angle Neutron Scattering. *Biomacromolecules* **2012**, *13* (10), 3355-3369.
5. Ferry, J. D., *Viscoelastic Properties of Polymers*. 3rd ed.; Wiley: 1980.
6. Larson, R. G., *Constitutive Equations for Polymer Melts and Solutions*. Butterworth-Heinemann: 2013.
7. Cox, W. P.; Merz, E. H., *Journal of Polymer Science* **1958**, *28*, 619-622.